# A 4-Element UWB MIMO Antenna System with High Isolation Performance

**Tongyu Ding[1], Haobin Yang[1], Zhiwei Chen[1], Zhen Lin[2], Bin He[2], and Chong-Zhi Han[1*]**

[1]School of Ocean Information Engineering
Jimei University, Xiamen, 361021, China
tyding@jmu.edu.cn, h.yang@jmu.edu.cn, chongzhi_han@jmu.edu.cn

[2]China Mobile Group Device Co., Ltd
Shenzhen, 518067, China

***Abstract –*** This paper proposes a 4-element multiple-input multiple-output (MIMO) antenna system, which is intended for ultra-wideband (UWB) applications. The antenna has a dimension of $92 \times 70 \times 1.6$ mm$^3$. It achieves element isolation via the defected ground structure (DGS) and symmetric E-shaped branch structures design. The realized operating bandwidth is from 3 GHz to 18 GHz, with 15 dB isolation within the whole wide band. The envelope correlation coefficient (ECC) is less than 0.01 with diversity gain (DG) greater than 9.95. The prototype is fabricated and measured to verify its potential applications for UWB MIMO communication.

***Index Terms –*** DG, ECC, isolation, MIMO, UWB.

## I. INTRODUCTION

The ultra-wideband (UWB) technology has been highly committed for decades due to low power consumption and high-speed data transmission [1–3], making it continuously promising technology in versatile future fields including indoor positioning [4], radar detection [5], and wireless communications [6–8]. As the demand for UWB applications increases, research and developments of UWB technologies and devices have attracted considerable attention.

More recently, multiple input multiple output (MIMO) technology has become one key technology of future mobile and wireless communication systems. It is worth noting that MIMO significantly improves the spectral efficiency of the UWB system. As a result, combining MIMO technologies in UWB design has become the main trend in UWB studies [9–10]. In this sense, research on UWB MIMO antennas has emerged as a hotspot in wireless communication system research. The combined use of UWB and MIMO technologies is anticipated to bring about new opportunities and challenges for UWB antennas [11].

The main challenge of UWB MIMO antennas in mobile terminals is achieving high isolation between antenna elements [12]. In [13, 14], neutralization line structures are used between antenna elements to reduce mutual coupling, while in [15–19], polarization diversity technology is used to achieve natural isolation. In [20–24], mutual coupling is reduced by using defected ground structures (DGS). For instance, [23] etches two novel bent slits into the ground plane and achieves -10 dB $S_{11}$ and -18 dB $S_{21}$ from 2.4 to 6.55 GHz. In addition, antenna elements isolation can also be improved by loading parasitic elements [25–28]. For instance, a parasitic T-shaped strip is used as a decoupling structure between the radiating elements in [28], enabling the antenna to operate from 3.08 to 11.8 GHz with 15 dB isolation. Electromagnetic band gap (EBG) structures are also considered [29–31]. The proposed EBG structures employ two closely coupled arrays, one comprising linear conducting patches and the other comprising apertures (slits) in the ground plane, to reduce the $S_{12}$ to values lower than -20 dB from 3.44 to 6.13 GHz [31]. All these techniques have proven useful for constructing different resonant structures corresponding to different frequencies. Since DGS is preferably used for improving decoupling while parasitic structures are more often used to broaden the bandwidth, this work combines these two techniques to design a MIMO antenna system meeting both requirements.

In this paper, a 4-element UWB MIMO antenna is designed and fabricated. For the element design, the proposed tapered fed hexagon-shaped patch microstrip is simulated and verified to achieve a wide operating band from 3 GHz to 10.6 GHz. A dual-element MIMO antenna is then constructed, and 15 dB isolation performance is achieved through DGS and parasitic branch structure. Furthermore, a 4-element MIMO antenna is realized where decoupling of the compact MIMO antenna is achieved through the design of two E-shaped branch structures. Simulation results show that the overall operating bandwidth of the system is further broadened up to 18 GHz. The isolation of

each two elements is greater than 15 dB. Section II describes the methodology of this work; it illustrates the design process from a single element to the 4-element array, as well as theoretical analysis and simulation verification. Section III shows the measured results as well as discussion, and Section IV concludes the paper.

## II. METHODOLOGY

### A. Design of the single-element UWB antenna

The configuration of the proposed UWB antenna element is presented in Fig. 1. It uses 1.6 mm thick FR4 ($\varepsilon_r = 4.4$) as the substrate. On top of the substrate, a hexagon-shaped radiated patch and a tapered feedline form a hexagon-shape monopole. On the bottom of the substrate, the ground plane is half cut off to form a DGS, which effectively improves the impedance matching bandwidth of the antenna. Detailed dimensions of the single-element antenna are given in Table 1.

In the process of impedance matching design, the evolution of the proposed UWB antenna is exhibited in Fig. 2. Simulated results of each step (shape of element patch transferred from sample $a$ to $d$) are illustrated in Fig. 3. The hexagon-shaped patch microstrip has better broadband characteristics (3 to 10.6 GHz) compared with other common microstrip patch shapes, such as rectangular, triangular, and circular shapes, because the hexagonal radiating patch owns more uniform electric field distribution at the edges of the antenna, which reduces edge effects and impedance changes.
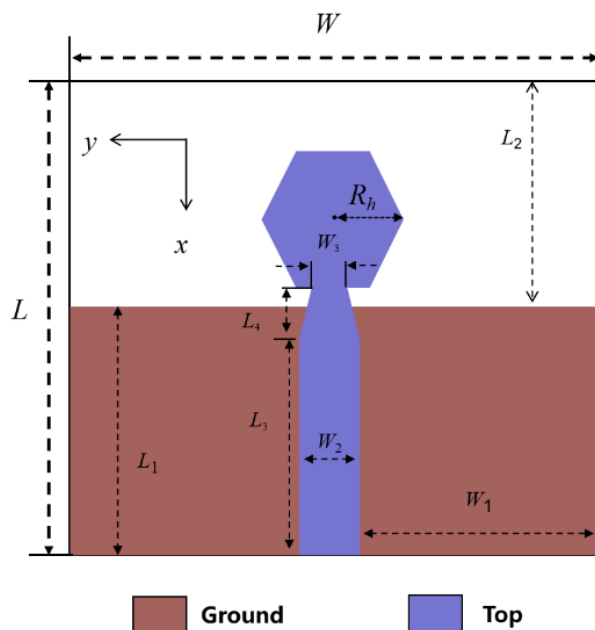
Table 1: Dimensions of the single-element antenna

| Par. | Value (mm) | Par. | Value (mm) |
|------|-----------|------|-----------|
| $L$ | 17.5 | $L_4$ | 5.77 |
| $W$ | 46 | $W_1$ | 10 |
| $L_1$ | 18.1 | $W_2$ | 3.01 |
| $L_2$ | 16.9 | $W_3$ | 2.01 |
| $L_3$ | 13.26 | $R_h$ | 7 |



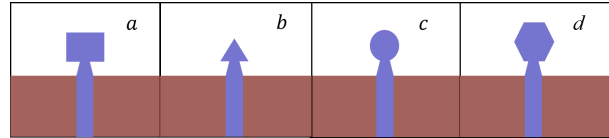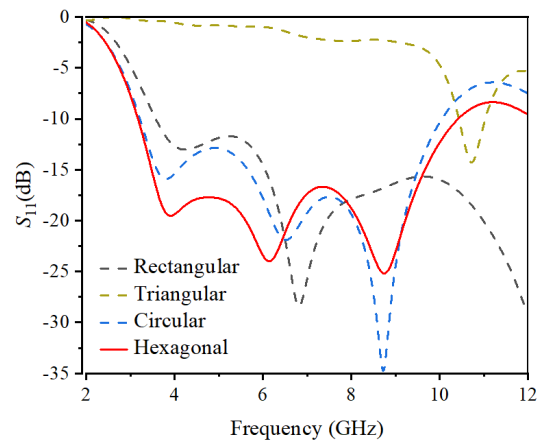Fig. 2. Evolution of a UWB antenna element.



Fig. 3. Simulated $S$-parameters of the four types of antenna element in Fig. 2.

### B. Design of dual-element UWB MIMO antenna

Since the single-element antenna has achieved satisfying bandwidth, we make one step further to develop a dual-element MIMO system. The configuration of the dual-element UWB MIMO antenna element is presented in Fig. 4. It uses 1.6 mm thick FR4 ($\varepsilon_r = 4.4$) as the substrate. On top of the substrate, two tapered feeds and two hexagonal radiating patches are arranged in parallel. On the bottom of the substrate, the ground plane uses etched rectangular slots to improve the mutual decoupling. It is found that the effect between the two elements changes the surface current and the electromagnetic field distribution near the feeding point, and therefore changes the impedance bandwidth. This dual-element antenna operates within a wide frequency range of 3-18 GHz. The dimensions of the dual-element antenna are given in Table 2.

In [32], the mentioned antenna system achieves 15 dB isolation (3.1-11.8 GHz) using parasitic branch
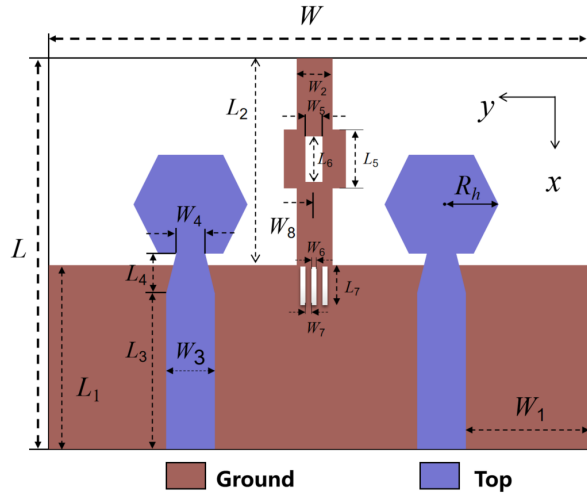


Fig. 1. Structure of the proposed antenna element.

Fig. 4. Dual-element UWB MIMO antenna.

Table 2: Dimensions of the dual-element antenna

| Par. | Value (mm) | Par. | Value (mm) | Par. | Value (mm) |
|---|---|---|---|---|---|
| $L$ | 35 | $L_5$ | 6 | $W_4$ | 2.01 |
| $W$ | 46 | $L_6$ | 5 | $W_5$ | 3 |
| $L_1$ | 18.1 | $L_7$ | 4 | $W_6$ | 0.5 |
| $L_2$ | 16.9 | $W_1$ | 10 | $W_7$ | 0.5 |
| $L_3$ | 13.26 | $W_2$ | 3.5 | $W_8$ | 1.5 |
| $L_4$ | 5.77 | $W_3$ | 3.01 | $R_h$ | 7 |

Table 3: The performance comparison of the 2-element antenna

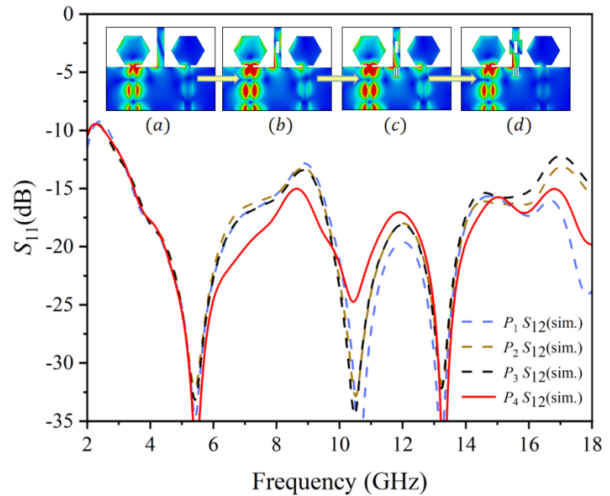| Ref | Size (mm) | Isolation (dB) |
|---|---|---|
| [32] | $38 \times 38 \times 1.6$ | >15 (3.1∼11.8 GHz) |
| [33] | $90 \times 40 \times 0.79$ | >17 (2.4∼4.2 GHz) |
| [34] | $50 \times 40 \times 1.6$ | >15 (2.5∼12 GHz) |
| [35] | $48 \times 48 \times 0.8$ | >18 (2.5∼12 GHz) |
| [36] | $78 \times 40 \times 1.6$ | >19 (2.4∼6.55 GHz) |
| Proposed | $46 \times 35 \times 1.6$ | >15 (3∼18 GHz) |



Fig. 5. The evolution of structure and surface current in the dual-element MIMO antenna.

structures. This method provides good isolation over a wider bandwidth. On the other hand, in [36], the described antenna system achieves 19 dB isolation (2.4-6.55 GHz) using DGS. This method offers better isolation compared to the method in [32], but over a narrower bandwidth. The proposed dual-element UWB MIMO antenna system in this paper utilizes both DGS and parasitic branch structures.

This design proposes a series of solutions to address the issue of mutual interference among multiple antennas in MIMO systems. Figure 5 illustrates the design process (from model $a$ to $d$) and evolution of $S$-parameters of the dual-element UWB antenna. The operating frequency range of all these setups are 3-18 GHz. From model $a$ $d$, a loop structure was realized by etching a rectangular groove in the metal strip to guide the surface current into the ground plane. Further improvement was achieved by etching three rectangular slots into the ground of $b$, resulting in the isolation ($S_{12}$) of the antenna elements greater than 15 dB at high frequencies (14-18 GHz). To ensure the isolation of the elements depicted in $c$ remained greater than 15 dB in the 7-10 GHz range, two rectangular metal stubs were added to the edge of the

$c$ metal strip. The final dual-element design is referred to as in $d$.

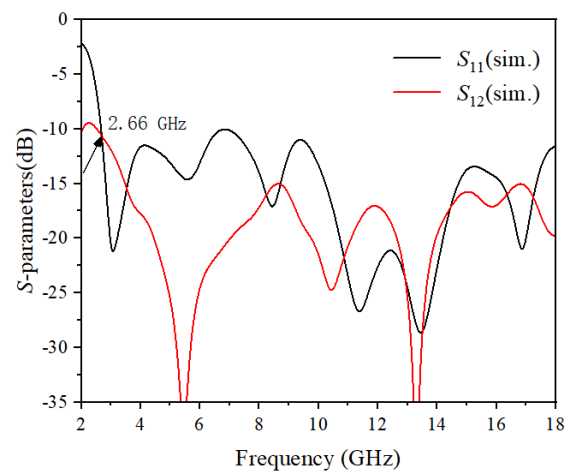The $S$-parameters for the dual-element UWB MIMO antenna are shown in Fig. 6. The operating frequency



Fig. 6. The $S$-parameters of the dual-element MIMO antenna.

range of the antenna meets the requirement of being less than -10 dB from 3 GHz to 18 GHz. The $S_{12}$ of the antenna remains less than -15 dB across the UWB frequency range, meeting the requirement of antenna isolation for MIMO systems.

## C. Design of 4-element UWB MIMO antenna

Based on the dual-element MIMO antenna, the final pattern of the proposed 4-element UWB MIMO system is realized and presented in Fig. 7. It has an overall size of $92 \times 70 \times 1.6mm^3$. On top of the FR4 substrate, the dual-element antenna pairs are placed symmetrically, while on the bottom, two E-shaped branch structures are designed to further improve the mutual decoupling. The operating bandwidth of the MIMO system is also 3-18 GHz, sufficiently meeting the wideband requirement. The dimensions of the quad-element antenna are given in Table 4.
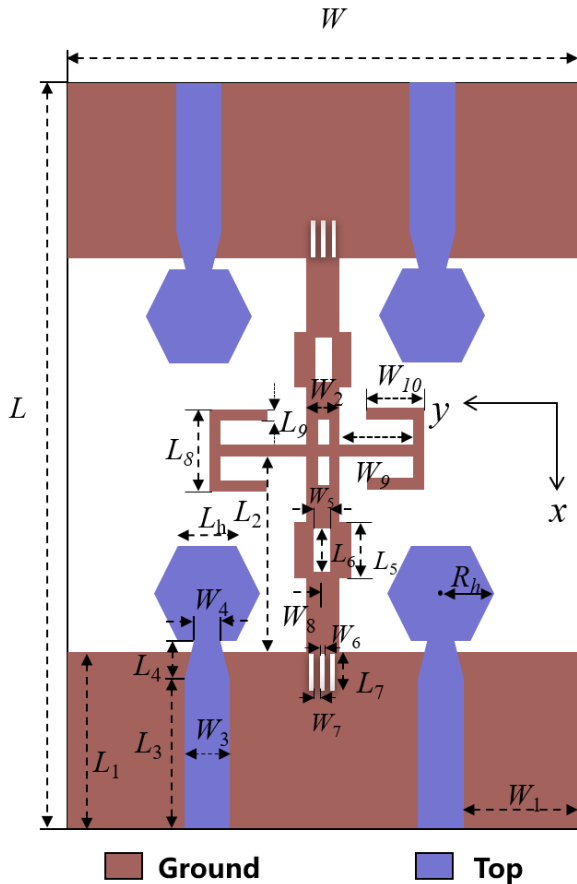
Table 4: Dimensions of the 4-element antenna

| Par. | Value (mm) | Par. | Value (mm) | Par. | Value (mm) |
|---|---|---|---|---|---|
| $L$ | 35 | $L_7$ | 4 | $W_6$ | 0.5 |
| $W$ | 46 | $L_8$ | 5 | $W_7$ | 0.5 |
| $L_1$ | 18.1 | $L_9$ | 0.5 | $W_8$ | 1.5 |
| $L_2$ | 16.9 | $W_1$ | 10 | $W_9$ | 5 |
| $L_3$ | 13.26 | $W_2$ | 3.5 | $W_{10}$ | 4 |
| $L_4$ | 5.77 | $W_3$ | 3.01 | $R_h$ | 7 |
| $L_5$ | 6 | $W_4$ | 2.01 | | |
| $L_6$ | 5 | $W_5$ | 3 | | |
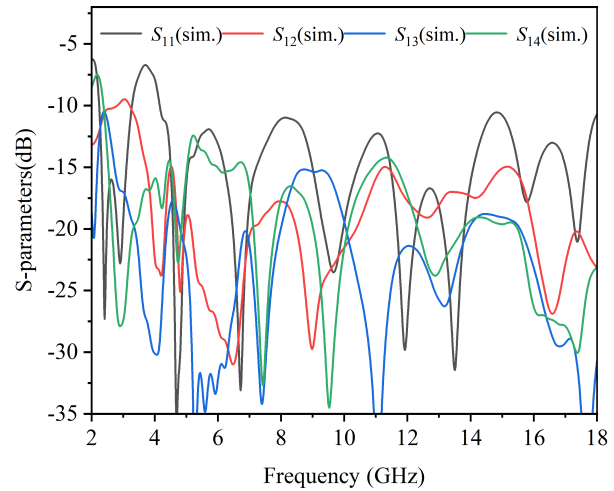


Fig. 8. The selected simulated $S$-parameters for the quad-element UWB MIMO antenna.



Fig. 7. Configuration of the 4-element MIMO antenna.

Through simulation of the proposed 4-element UWB MIMO antenna, the $S$-parameters in Fig. 8 are obtained and discussed. It is clear that $S_{11}$ is less than -10 dB from 3 GHz to 18 GHz. On the whole operating band, the isolation degree of arbitrary two elements reach more than 15 dB, indicating that the mutual coupling between the four elements is effectively suppressed. One of the key advantages of this system is its ability to achieve a 15 dB isolation range of operating (3-18 GHz) frequency.

When one port is excited and the other three ports are terminated, the surface current distribution is simulated at 5 GHz, 10 GHz, and 15 GHz, respectively, as shown in Fig. 9. The design of E-shaped branches between the two dual-element MIMO antenna pairs forms current loops, and the current generated by the radiation patch flows into the ground plane through the rectangular metal strip. This effectively reduces the coupling between the four antenna elements, resulting in good independence between the antenna elements and achieving the expected isolation.

The total efficiency of the 4-element UWB MIMO antenna is shown in Fig. 10; the simulated efficiency value within the whole operating band testifies to the functionality and applicability of the proposed system.
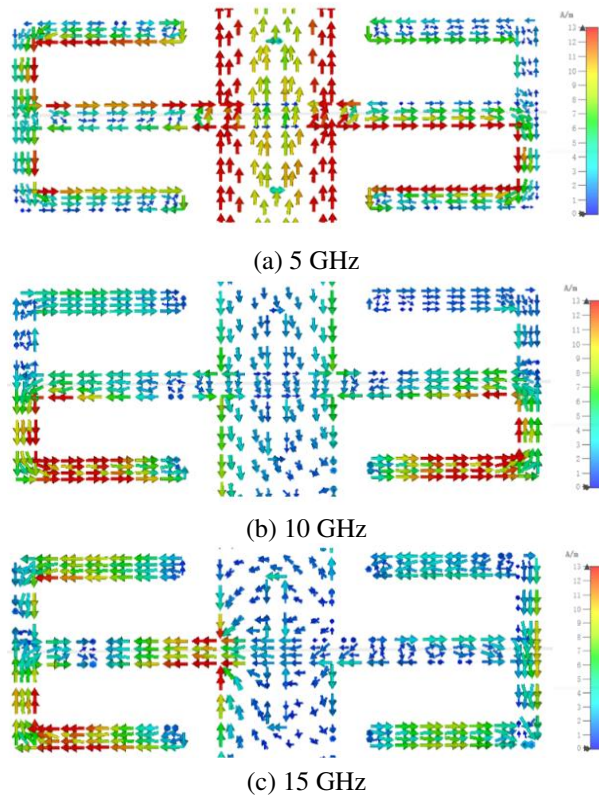
(a) 5 GHz



(b) 10 GHz



(c) 15 GHz

Fig. 9. Surface current distribution of the 4-element UWB MIMO antenna at (a) 5 GHz, (b) 10 GHz, and (c) 15 GHz.
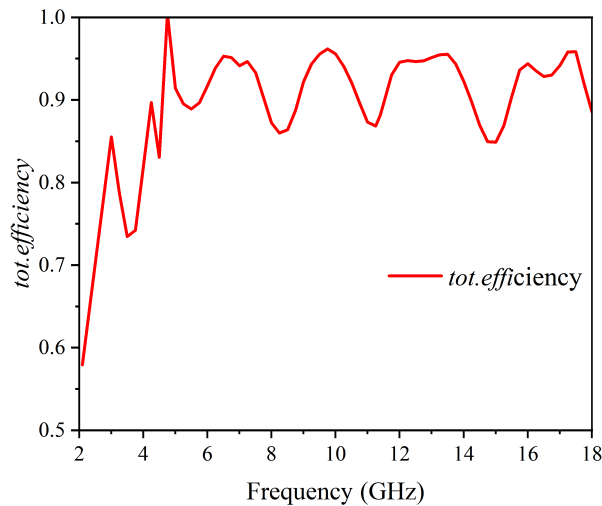


Fig. 10. The total efficiency of the 4-element UWB MIMO antenna.

The four-element MIMO antenna system can enhance the capacity and data rates of wireless communication systems. It enables improved signal quality, increased spectral efficiency, and enhanced cover-

age, making it suitable for applications such as 5G and beyond.

## III. MEASUREMENT AND DISCUSSION

Figure 11 shows a snapshot of the fabricated model of the proposed UWB MIMO antenna, with Fig. 11 (a) representing the front side view of the antenna and Fig. 11 (b) representing the back side view of the antenna. Through measurements of the fabricated prototype, Fig. 12 shows the comparison between simulated and measured data of the MIMO antenna's $S$-parameters. The measurements demonstrate that the bandwidth and isolation of the proposed antenna closely match the simulations. The operating bandwidth is from 3 GHz to 18 GHz with a 15 dB isolation performance, indicating that the design of the MIMO system does not affect the radiation characteristics of the UWB antenna.

The envelope correlation coefficient (ECC) quantifies the correlation between signals transmitted from different wireless communication channels and received by antennas, reflecting the degree of coupling in MIMO antennas. A lower ECC value indicates less coupling between ports, which is desirable for achieving high diversity performance. ECC values below 0.5 are typically preferred. ECC can be calculated using the scattering $S$-parameter, with the formula

$$ECC = \frac{\left| S_{ii}^* S_{ij} + S_{ji}^* S_{jj} \right|^2}{\left| \left( 1 - |S_{ii}|^2 - |S_{ji}|^2 \right) \cdot \left( 1 - |S_{jj}|^2 - |S_{ij}|^2 \right) \right|}. \quad (1)$$
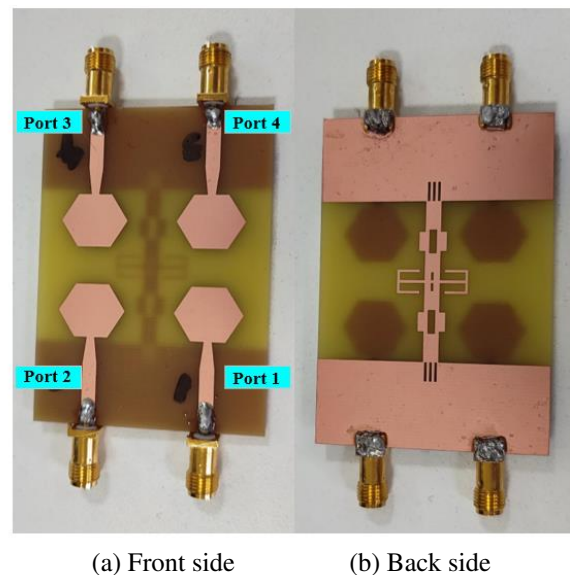


(a) Front side          (b) Back side

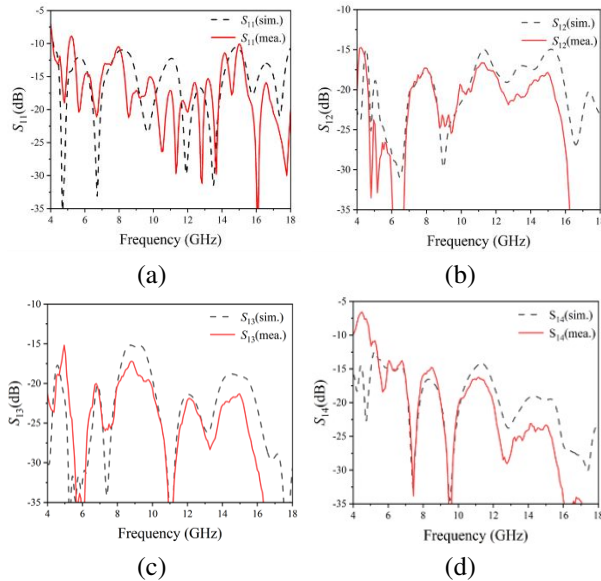Fig. 11. Snapshot of fabricated prototype of the 4-element UWB MIMO antenna: (a) Front view and (b) back view.

Fig. 12. Measurement and simulation results of the $S$-parameter for this 4-element MIMO antenna: (a) $S_{11}$, (b) $S_{12}$, (c) $S_{13}$, and (d) $S_{14}$.

Diversity gain (DG) is a key metric for evaluating diversity performance. A higher diversity gain is achieved when there is less correlation among the antenna elements. The relationship between DG and ECC is illustrated in equation (2):

$$DG = 10 \times \sqrt{1 - |ECC|}. \qquad (2)$$

These two parameters are calculated in this work according to (1) and (2), as shown in Fig. 13, where the ECC performance is less than 0.01 and DG is greater than 9.95.

The overall data comparison shows excellent agreement between the measured results and the simulation results, indicating good isolation and high gain cha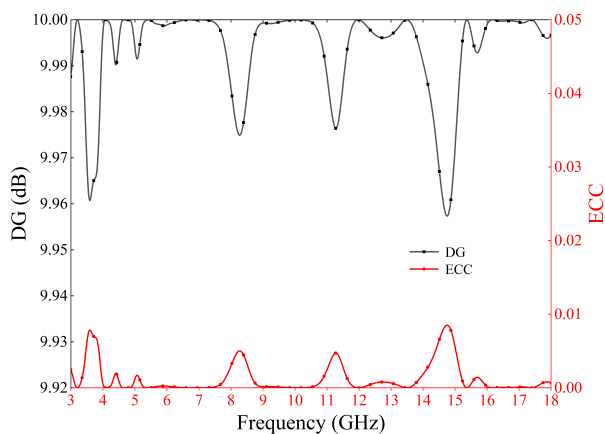racteristics of the antenna. Furthermore, the ingenious and novel structure confirms the proposed antenna as a desirable candidate for UWB-MIMO applications.

## IV. CONCLUSION

In this paper, a four element UWB-MIMO antenna with DGS and parasitic decoupling structures is proposed and analyzed. The antenna is operatable from 3 GHz to 18 GHz, which is a superior wide operating band. Design of decoupling structures such as multiple slots, stubs, and E-shaped symmetric strips achieves a 15 dB high isolation within the ultrawide operating band. Simulated total efficiency is greater than 0.8 and the ECC is less 0.01, whereas DG is greater than 9.95 across the frequency range. Simulations and measurements agree well and show that the proposed antenna is a good candidate for the UWB-MIMO applications.

## ACKNOWLEDGMENT

Fig. 13. ECC and DG results of the MIMO antenna.

## REFERENCES

[1] M. NejatiJahromi, M. N. Jahromi and M. Rahman, "A new compact planar antenna for switching between UWB, narrow band and UWB with tunable-notch behaviors for UWB and WLAN applications," *Appl. Comput. Electromagn. Soc.*, vol. 33, pp. 400-406, 2021.

[2] S. Park and K. Y. Jung, "Novel compact UWB planar monopole antenna using a ribbon-shaped slot," *IEEE Access*, vol. 10, pp. 61951-61959, 2022.

[3] Y. Yang, Z. Zhao, X. Ding, Z. Nie, and Q.-H. Liu, "Compact UWB slot antenna utilizing traveling-wave mode based on slotline transitions," *IEEE Trans. Antennas Propagat.*, vol. 67, no. 1, pp. 140-150, 2019.

[4] S. Sung, H. Kim, and J.-I. Jung, "Accurate indoor positioning for UWB-based personal devices using deep learning," *IEEE Access,* vol. 11, pp. 20095-20113, 2023.

[5] Y. K. Wang, L. Li, X. Y. Zhou, and T. J. Cui, "Supervised Automatic Detection of UWB ground-penetrating radar targets using the regression SSIM measure," *IEEE Geoscience Remote Sens. Letters*, vol. 13, no. 5, pp. 621-625, 2016.

[6] T. Mavridis, J. Sarrazin, L. Petrillo, P. De Doncker, and A. Benlarbi-Delaï, "Information spatial focusing scheme for UWB wireless communications in smart environments," *IEEE Antennas Wirel. Propagat. Lett.*, vol. 14, pp. 20-23, 2015.

[7] K. Bahadori and Y. Rahmat-Samii, "A miniaturized elliptic-card UWB antenna with WLAN band rejection for wireless communications," *IEEE*

*Transactions Antennas Propagat.*, vol. 55, no. 11, pp. 3326-3332, 2007.

[8] B. Zhou, F. Chen, W. Rhee, and Z. Wang, "A reconfigurable FM-UWB transceiver for short-range wireless communications," *IEEE Microwave Wirel. Comput. Lett.*, vol. 23, no. 7, pp. 371-373, July 2013.

[9] G. Srivastava and A. Mohan, "Compact MIMO slot antenna for UWB applications," *IEEE Antennas Wirel. Propagat. Lett.*, vol. 15, pp. 1057-1060, 2016.

[10] M. Naser-Moghadasi, H. Rousta, and B. S. Virdee, "Compact UWB planar monopole antenna," *IEEE Antennas Wirel. Propagat. Lett.*, vol. 8, pp. 1382-1385, 2009.

[11] W. K. Toh, X. Qing, and Z. N. Chen, "A planar UWB patch-dipole antenna," *IEEE Trans. Antennas Propagat.*, vol. 59, no. 9, pp. 3441-3444, Sep. 2011.

[12] L. Y. Nie, X. Q. Lin, Z. Q. Yang, J. Zhang, and B. Wang, "Structure-shared planar UWB MIMO antenna with high isolation for mobile platform," *IEEE Trans. Antennas Propagat.,* vol. 67, no. 4, pp. 2735-2738, 2019.

[13] A. Mohanty and B. R. Behera, "Investigation of 2-port UWB MIMO diversity antenna design using characteristics mode analysis," *AEU – I. J. Electron Commun.*, vol. 124, p. 153361, 2020.

[14] A. Kayabasi, A. Toktas, E. Yigit, and K. Sabanci, "Triangular quad-port multi-polarized UWB MIMO antenna with enhanced isolation using neutralization ring," *AEU – I. J. Electron Commun.,* vol. 85, pp. 47-53, 2018.

[15] A. S. Eltrass and N. A. Elborae, "New design of UWB-MIMO antenna with enhanced isolation and dual-band rejection for WiMAX and WLAN systems," *IET Microwaves Antennas*, vol. 13, pp. 683-691, 2019.

[16] M. M. Hassan, M. Rasool, M. U. Asghar, Z. Zahid, A. A. Khan, I. Rashid, A. Rauf, and F. A. Bhatti, "A novel UWB MIMO antenna array with band notch characteristics using parasitic decoupler," *J. Electromagn. Waves Appl.*, vol. 34, no. 9, pp. 1225-1238, 2020.

[17] Y. I. Nechayev, C. C. Constantinou, X. Wu, and P. S. Hall, "De-polarization of on-body channels and polarization diversity at 60 GHz," *IEEE Trans. Antennas Propagat.*, vol. 62, no. 12, pp. 6519-6523, 2014.

[18] K. Wei, B. Zhu, and M. Tao, "The circular polarization diversity antennas achieved by a fractal defected ground structure," *IEEE Access*, vol. 7, pp. 92030-92036, 2019.

[19] S. Hiraoka, Y. Nakashima, T. Yamazato, S. Arai, Y. Tadokoro, and H. Tanaka, "Interference-aided detection of subthreshold signal using beam control in polarization diversity reception," *IEEE Commun. Lett.*, vol. 22, no. 9, pp. 1926-1929, 2018.

[20] P. Kumar, S. Pathan, S. Vincent, O. P. Kumar, N. Washwanth, P. Kumar, P. R. Shetty, and T. Ali, "A compact quad-port UWB MIMO antenna with improved isolation using a novel mesh-like decoupling structure and unique DGS," *IEEE Transactions on Circuits and Systems II: Express Briefs*, vol. 70, no. 3, pp. 949-953, 2023.

[21] R. Gómez-Villanueva and H. Jardón-Aguilar, "Compact UWB uniplanar four-port MIMO antenna array with rejecting band," *IEEE Antennas Wirel. Propagat. Lett.*, vol. 18, no. 12, pp. 2543-2547, 2019.

[22] P. Kumar, S. Pathan, S. Vincent, O. P. Kumar, N. Washwanth, P. Kumar, P. R. Shetty, and T. Ali, "Design of a six-port compact UWB MIMO antenna with a distinctive DGS for improved isolation," *IEEE Access*, vol. 10, pp. 112964-112974, 2022.

[23] J.-F. Li, Q.-X. Chu, and T.-G. Huang, "A compact wideband MIMO antenna with two novel bent slits," *IEEE Trans. Antennas Propagat.*, vol. 60, no. 2, pp. 482-489, 2012.

[24] T. Shabbir, R Saleem, A. Akram, and F. Shafique, "UWB-MIMO quadruple with FSS-inspired decoupling structures and defected grounds," *Applied Computational Electromagnetics Society (ACES) Journal*, vol. 30, pp. 84-190, 2021.

[25] K. Phaebua, C. Phongcharoenpanich, D. Torrungrueng, N. Surittikul, and W. Villarroel, "An eight-branch folded strip antenna with a circular parasitic patch on circular ground plane for SDARS application," *2009 IEEE Antennas Propagat. Soc. Inter. Sym.*, pp. 1-4, 2009.

[26] P.-H. Deng, M.-W. Li, W.-T. Chen, C.-H. Lin, C.-H. Lu, R.-T. Tsai, and K.-H. Chen, "Designs of branch-line couplers by considering the parasitic effects of P-I-N diodes," *IEEE Access*, vol. 8, pp. 223089-223100, 2020.

[27] P. Jha, A. Kumar, A. De, and R. K. Jain, "Super ultra-wideband planar antenna with parasitic notch and frequency selective surface for gain enhancement," *Applied Computational Electromagnetics Society (ACES) Journal*, vol. 37, pp. 757-764, 2022.

[28] L. Kang, H. Li, X. Wang, and X. Shi, "Compact offset microstrip-fed MIMO antenna for band-notched UWB applications," *IEEE Antennas Wirel. Propagat. Lett.,* vol. 14, pp. 1754-1757, 2015.

[29] S. Barth and A. K. Iyer, "The MTM-EBG as a rigorous multiconductor model of the UC-EBG and approaches for miniaturization," *IEEE Trans. Antennas Propagat.,* vol. 70, no. 4, pp. 2822-2831, 2022.

[30] M. Kashani, L. Shafai, and D. Isleifson, "Truncated and suspended microstrip patch antennas over an EBG ground plane," *IEEE 19th International Symposium Antenna Technology Applied Electromagnetics*, Winnipeg, MB, Canada, pp. 1-2, 2021.

[31] Q. Li, A. P. Feresidis, M. Mavridou, and P. S. Hall, "Miniaturized double-layer EBG structures for broadband mutual coupling reduction between UWB monopoles," *IEEE Trans. Antennas and Propagat.*, vol. 63, no. 3, pp. 1168-1171, 2015.

[32] L. Kang, H. Li, X. Wang, and X. Shi, "Compact offset microstrip-fed MIMO antenna for band-notched UWB applications," *IEEE Antennas and Wireless Propagation Letters*, vol. 14, pp. 1754-1757, 2015.

[33] C. H. See, R. A. Abd-Alhameed, and Z. Z. Abidin, "Wideband printed MIMO/diversity monopole antenna for Wi Fi/Wi MAX applications," *IEEE Transactions on Antennas and Propagation,* pp. 2028-2035, 2012.

[34] G. Lin, C. Sung, J. Chen, and M. Hung, "Isolation improvement in UWB MIMO antenna system using carbon black film," *IEEE Antennas and Wireless Propagation Letters*, pp. 222-225, 2017.

[35] P. Gao, S. He, X. Wei, and Z. Xu, "Compact printed UWB diversity slot antenna with 5.5-GHz band-notched characteristics," *IEEE Antennas and Wireless Propagation Letters*, pp. 376-379, 2014.

[36] J. Li, Q. Chu, and T. Huang. "A compact wideband MIMO antenna with two novel bent slits," *IEEE Transactions on Antennas and Propagation*, vol. 60, no. 2, pp. 482-489, 2012.

**Tongyu Ding** was born in Heilongjiang, China in 1987. He received the M.S. degree from Harbin Institute of Technology, China and the Ph.D. degree in electronics and communication engineering from the Politecnico di Torino, Italy, in 2011 and in 2015, respectively. Currently he is an associate professor with the School of Ocean Information Engineering, Jimei University. His recent research interests include antennas, RIS, and numerical techniques for 5G wireless communications.

**Haobin Yang** was born in Sichuan, China. He obtained his bachelor's degree from Jimei University, Xiamen, China, in 2023. Currently, he is pursuing a master's degree at Jimei University. His main research focus is on reconfigurable intelligent surfaces.

**Zhiwei Chen** was born in Fujian, China. He enrolled in Jimei University in 2021 and is currently working toward the bachelor's degree at the School of Ocean Information Engineering. His recent research interest is UWB MIMO antennas.

**Zhen Lin** graduated from the Department of Electronic and Communication Engineering, South China University of Technology, in 2000. He joined China Mobile in 2004. In 2019, he received his doctor's degree in administration from Huazhong University of Science and Technology. Currently, he is the general manager of R&D Center of China Mobile Communications Group Terminal Co., LTD., mainly engaged in the R&D management of terminal software and hardware in the field of smart home.

**Bin He** graduated from the Institute of Computing Technology, Chinese Academy of Sciences in 2005 with a master's degree. He is currently the deputy general manager of the R&D Center of China Mobile Communications Group Terminal Co., LTD., engaged in the research and development of intelligent terminal products hardware and software and related platforms.

**Chong-Zhi Han** received the B.E. degree and the M.Eng. degree in electronic information engineering from Harbin Institute of Technology, Harbin, China. In 2020, he received the Ph.D. degree in Shenzhen University, Shenzhen, China. Currently he is an associate professor with the School of Ocean Information Engineering, Jimei University. His current research interests include the development and application of MIMO antennas and millimeter wave antennas.